Postprint of: Zaborowska E., Lu X., Makinia J., Strategies for mitigating nitrous oxide production and decreasing the carbon footprint of a full-scale combined nitrogen and phosphorus removal activated sludge system, Water Research, Vol. 162 (2019), pp. 53-63, DOI: 10.1016/j.watres.2019.06.057

Strategies for mitigating nitrous oxide production and decreasing the carbon footprint of a full-scale combined nitrogen and phosphorus removal activated sludge system

Ewa Zaborowska[1], *Xi Lu*[1,2]*, *Jacek Makinia*[1]

[1] Faculty of Civil and Environmental Engineering, Gdansk University of Technology, Narutowicza street 11/12, 80-233 Gdansk, Poland

[2] Institute of Environmental Science and Technology, Tongji University, 1239 Siping Road, Yangpu District, Shanghai 200092, China

(*corresponding author: Xi Lu; tel: +86 15316633129; email: 1310446_lucy@tongji.edu.cn)

ABSTRACT

Nitrous oxide (N_2O) emitted from biological nutrient removal activated sludge systems contributes significantly to the total carbon footprint of modern wastewater treatment plants. In the present study, N_2O production and emissions were experimentally determined in a large-scale plant (220,000 PE) employing combined nitrogen (N) and phosphorus (P) removal. As a modelling tool, the Activated Sludge Model 2d (ASM2d) was extended with modules describing multiple N_2O production pathways and N_2O liquid-gas transfers. The new model

was calibrated and validated using the results of laboratory experiments and full-scale measurements. Different operational strategies were evaluated following the proposed model-based procedure. Heterotrophic denitrification was found to be the predominant pathway of N_2O production under both anoxic and aerobic conditions. This behaviour could primarily be attributed to the predominant abundance of heterotrophic denitrifiers over nitrifiers. Simulations revealed that the optimal solution for minimizing liquid N_2O production is to set the dissolved oxygen concentration in the aerobic zone from 1 to 2 mg O_2/L and to enhance the mixed liquor recirculation rate (MLR) (> 500% of the influent flowrate) while not compromising effluent standards. Regarding the actual conditions, the potential reduction in the carbon footprint was estimated to be 10% by applying the proposed operational strategy. The results suggest that considerable improvements can be achieved without substantial upgrades and increased costs.

KEYWORDS

Carbon footprint; full-scale plant; nitrous oxide; N_2O mitigation; modelling

1. Introduction

Nitrous oxide (N_2O) emissions from anthropogenic sources have received special attention in recent years. As it is reported by the Intergovernmental Panel on Climate Change (IPCC, 2014), the global warming potential (GWP) of N_2O is 265 times greater than that of carbon dioxide (CO_2). In modern wastewater treatment plants (WWTPs), up to 90% of N_2O can be produced and subsequently emitted in the biological steps via the nitrification and denitrification

processes (Campos et al., 2016). Recent investigations have identified three microbial pathways for N_2O production (Schreiber et al., 2012; Tallec et al., 2006; Wunderlin et al., 2012). Two pathways are mediated by autotrophic nitrifiers, specifically ammonia oxidizing bacteria (AOB), including the hydroxylamine (NH_2OH) oxidation and autotrophic denitrification. The third pathway is related to heterotrophic denitrification with N_2O as an intermediate product. The conditions favouring N_2O production consist of low dissolved oxygen (DO) levels during nitrification, low carbon to nitrogen (C/N) ratios during heterotrophic denitrification, and elevated nitrite (NO_2^--N) levels during both nitrification and denitrification (Flores-Alsina et al., 2011; Mannina et al., 2017; Massara et al., 2018; Ni et al., 2011; Peng et al., 2014; Tallec et al., 2008). In general, aerobic conditions contribute to higher N_2O production through the nitrification-related pathways and to higher N_2O emissions due to stripping. Furthermore, intensive aerobic conditions are also responsible for increased energy requirements and an increased carbon footprint (Kim et al., 2015; Massara et al., 2018; Mikosz, 2016; Rodriguez-Caballero et al., 2015).

Numerous full-scale measurements on N_2O emissions have been conducted worldwide (Table S1), but considerable variations (one order of magnitude) have been observed both across different plants and temporarily within one plant (Daelman et al., 2015; Ni et al., 2015; Pan et al., 2016). Several measures for mitigating N_2O emissions have been proposed, including the step-aeration mode (Wang et al., 2016), distribution of the return activated sludge between compartments (Pan et al., 2016), controlling the DO concentrations (Sun et al., 2015), and cancelling the anaerobic phase and extending the idle phase in a sequencing batch reactor

(Chen et al., 2014). It should be emphasized that N_2O emissions need to be accurately estimated due to the potential impact on the total carbon footprint of a WWTP. De Haas and Hartley (2004) estimated that just 1% of the removed N load emitted as N_2O would increase the carbon footprint of a plant by approximately 30%. The reported contributions of N_2O emissions to the total carbon footprint ranged from 60 to 80% (Daelman et al., 2013; Rodriguez-Caballero et al., 2015). Regardless of these differences, mitigating N_2O emissions and decreasing the carbon footprint of WWTPs is strongly linked to the energy consuming processes in the bioreactors, such as aeration and pumping (Marques et al., 2016; Pan et al., 2016). Modification of the operational conditions of existing plants is thus the most economical way to decrease greenhouse gas (GHG) emissions provided that the effluent quality is not degraded (Campos et al., 2016; Kim et al., 2015; Mikosz, 2016).

Selection of the optimal operational conditions in bioreactors with respect to GHG emissions, energy and effluent quality becomes a complex multivariable optimization problem (Kim et al., 2015) that can be solved by model-based analysis. Multi-pathway N_2O production models have been developed and evaluated under laboratory conditions, including identification of the dominant N_2O production pathways (Massara et al., 2017; Ni and Yuan, 2015). However, for practical applications in full-scale bioreactors, it has been postulated that these models should be extended by considering the liquid-gas transfers of N_2O to predict N_2O emissions (Massara et al., 2017). Only in a few studies (Ni et al., 2013; Ni et al., 2015; Blomberg et al., 2018) conducted in N removal (nitrification-denitrification) activated sludge (AS) systems, comprehensive full-scale monitoring data have been used to evaluate the N_2O production and

emission models. Until now, no modelling studies have been performed for full-scale combined N and P removal systems, which are most commonly employed in modern WWTPs. Mathematical models describing N_2O production during the enhanced biological P removal (EBPR) process have recently been proposed (Liu et al., 2015; Massara et al., 2018; Wisniewski et al., 2018), but these models have not yet been evaluated against the full-scale experimental data.

In the present study, N_2O production and emissions were experimentally determined and predicted for a large-scale municipal WWTP located in the city of Slupsk (northern Poland), employing combined N and P removal. In the modelling part of the study, the Activated Sludge Model 2d (ASM2d) (Henze et al., 2000) was extended with modules describing multi-pathway N_2O production and N_2O liquid-gas transfers. The new model was then calibrated and validated using the results of extensive laboratory-scale experiments and full-scale measurement campaigns, performed in different periods, in the studied facility. For the model-based evaluation of N_2O production and emission, a standardized procedure was proposed, including the analysis of N_2O mitigation strategies and carbon footprint calculation. Following that procedure, the optimal operational parameters were determined with respect to both direct and indirect GHG emissions at the studied plant. The model developed in the present study combines and evaluates against the full-scale experimental data all known aspects related to N_2O behaviour in biological nutrient removal (BNR) WWTPs, including the three known pathways of N_2O production for N transformations, the role of denitrifying polyphosphate accumulating organisms (DPAO) in denitrification, and N_2O liquid-gas transfers.

2. Materials and methods

2.1. Characteristics of the study site

The studied WWTP is a large facility (220,000 PE) treating municipal wastewater from the city of Slupsk (northern Poland) and surrounding communities. The biological step of the studied plant consists of three parallel lines operated in an A_2O (anaerobic/anoxic/oxic) configuration. A simplified schematic layout of a single line and the dimensions of each compartment are shown in Figure 1. The internal mixed liquor recirculation (MLR) is returned from the last aerobic compartment (AE2) to the second or the third compartment in the bioreactor (AO1 or AO2, respectively), depending on the actual operating conditions. The return activated sludge (RAS) flow from the secondary clarifier is returned to the inlet of the bioreactor.

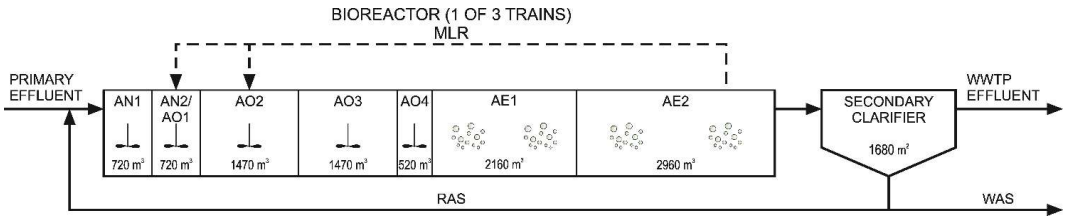

Figure 1. Schematic diagram of the biological step at the Slupsk WWTP (AN – anaerobic zone, AO – anoxic zone, AE – aerobic zone, WAS – waste activated sludge)

2.2. General procedure

A general procedure for model-based evaluation of N_2O production and emissions was developed and applied specifically to the studied WWTP (Figure S1 in the Supporting

Information (SI)). The procedure, tailored for the plant to maximize use of available data, incorporates the sequential steps from the full-scale and laboratory-scale (trials no. 1 and 2) data collection, through model development, calibration and validation, to the model-based evaluation of strategies for mitigating N_2O production and decreasing the carbon footprint. A two-step calibration was specifically applied for the N_2O data (i.e., calibration of N_2O production after achieving good fits for NH_4^+-N, NO_2^--N, and NO_3^--N) as proposed by Ni et al. (2015) and Domingo-Félez et al. (2017).

2.3. Collection of experimental data

2.3.1. Full-scale measurements

To maximize the use of available data for the studied plant, the results from two measurement campaigns were used for simulations. The campaigns were performed in the summer periods of different years (namely, 2012 and 2016), but the process conditions in terms of wastewater characteristics and aeration control, were similar in those periods (Table S2 in the SI). The average nominal hydraulic retention times in the bioreactor were 1.5 d and 1.7 d, respectively, in summer 2012 and summer 2016. With this approach, it could be confirmed if the model was capable of predicting performance for different periods with one set of parameters.

The first 4-day measurement campaign was performed in the biological reactor of the Slupsk WWTP in August 2012 at T = 20°C and total solids retention time (SRT) = 26 d. Grab samples were withdrawn every 2 h from the following sampling locations: primary effluent, and the anaerobic, anoxic and aerobic compartments in the bioreactor. The samples were analysed for

several parameters, including (i) chemical oxygen demand (COD), sCOD (soluble fraction of COD), total nitrogen (TN), total phosphorus (TP) for the primary effluent only and (ii) ammonia (NH_4^+-N), nitrate (NO_3^--N) and soluble ortho-phosphate (PO_4^{3-}-P) for all sampling points. The first 4-day campaign (trial no. 1, full-scale) was used for model calibration without consideration of N_2O data (as N_2O was not measured during that campaign). More details about that measurement campaign can be found in Zaborowska et al. (2017).

The second 4-day measurement campaign was conducted in the Slupsk WWTP in September 2016 at T = 21°C. Grab samples were withdrawn every 2 h from the following sampling points: plant influent, anaerobic, anoxic and aerobic compartments of the bioreactor. The plant influent was analysed for COD, sCOD, total suspended solids (TSS), volatile suspended solids (VSS), TN, total Kjeldahl nitrogen (TKN), NH_4^+-N, PO_4^{3-}-P and TP. The filtered samples of the mixed liquor from the bioreactors were analysed for NH_4^+-N, NO_3^--N and PO_4^{3-}-P. Moreover, average daily samples were also collected from the plant influent and from the primary and secondary effluents. The samples were analysed for a number of parameters, including COD, sCOD, TSS, VSS, TP, PO_4^{3-}-P, TN, TKN, NH_4^+-N, and NO_3^--N (only in the secondary effluent). The liquid and gaseous N_2O concentrations were continuously monitored during the campaign. The influent and effluent flowrates and DO concentrations in the first and the second aerobic zones (AE1 and AE2) were continuously measured and recorded every 10 min. The mixed liquor suspended solids (MLSS) and its volatile fraction (MLVSS) concentrations were measured once per day from grab samples withdrawn from AE2. The second measurement campaign

involving the liquid and gaseous N_2O measurements (trial no. 2, full-scale) was used for the full-scale model validation.

2.3.2. Laboratory measurements

A few accompanying laboratory-scale experiments were performed by using the biomass from the Slupsk WWTP in a 4 L laboratory-scale batch reactor at the controlled temperature T = 20 (± 0.5)°C. During the course of the experiments, the DO concentrations and temperatures were continuously monitored using a CellOx 325 probe (WTW, Germany) and were recorded every 20 s. The MLSS and MLVSS concentrations were measured at both the beginning and end of each experiment. Details on the analytical methods used in the experiments can be found in the SI.

One-phase (anoxic) and two-phase (anaerobic-aerobic/anoxic) experiments. One one-phase (anoxic) and two two-phase (anaerobic-aerobic/anoxic) experiments accompanied the first full-scale measurement campaign (trial no. 1, full-scale). More details about these experiments can be found in Zaborowska et al. (2017). These experimental data (trial no. 1, laboratory-scale) were used for the model calibration without consideration of N_2O data.

One-phase (aerobic) experiments with the liquid N_2O measurements. Two aerobic experiments, extended with the continuous liquid N_2O monitoring, accompanied the second full-scale measurement campaign (trial no. 2 full-scale). The 6-hour experiments were conducted at two different DO levels (DO = 1.0 mg O_2/L and DO = 0.5 mg O_2/L). To minimize the influence of

denitrification, the remaining nitrate in the mixed liquor was reduced before the experiments by adding sodium acetate (CH_3COONa) at 6 gCOD/gN. Only NH_4^+-N and $NaHCO_3$ (2 mole $NaHCO_3$ per mole NH_4^+-N) were supplied at the beginning of the experiment. During the experiments, NH_4^+-N, NO_2^--N and NO_3^--N were measured at a frequency of 30-60 min. The N_2O-N concentrations in the liquid phase were continuously monitored every 20s. These experimental data (trial no. 2, laboratory-scale) were used for model recalibration with consideration of N_2O data.

2.3.3. Measurements of N_2O concentration during the laboratory experiments and the full-scale measurement campaign

During the laboratory-scale experiments (trial no. 2), a Clark-type N_2O microsensor (Unisense Environment A/S, Denmark) was placed in the batch reactor. During the second full-scale measurement campaign (trial no. 2), the same N_2O microsensor was placed in a closed mobile reactor (V = 3 L), equipped with a mixer. The off-line location protected the sensor from undesirable displacements and ensured stable operation for the course of the experiment. The reactor was permanently fully filled (to avoid additional stripping effects) and was continuously fed with the mixed liquor by a lifting pump submerged 1 m below the water level. During the 4-day campaign, the sampling point was located in AE1. The liquid N_2O-N concentrations were continuously monitored and recorded every 20s. The basic characteristics of the microsensor and the temperature correction formula for the microsensor signal are described in detail in the SI.

The N_2O concentrations in the off-gas were measured by Fourier transform infrared (FTIR) gas analyser (Gasmet CX 4000) coupled with a flow meter and a floating hood located at the same sampling point as for the liquid N_2O. The frequency of sampling was set to 20 s. Data reported in the literature (Ni et al., 2015; Pan et al., 2016; Rodriguez-Caballero et al., 2014) revealed different longitudinal N_2O profiles along the aerobic compartment. The highest N_2O emissions correlated with either high NH_4^+-N and NO_2^--N concentrations or were attributed to process disturbances, such as no aeration periods or nitrification instability. In the present study, the selected location was assumed based on the results of both preliminary simulations and short-term N_2O measurements in different points in the bioreactor. The simulations revealed that approximately 70% of the total N_2O emissions from the bioreactor occurred in AE1. Moreover, in the field off-gas measurements, the N_2O concentrations (14.8±1.4 mg N/m^3) in AE1 were approximately 3 times greater when compared to those in AE2.

2.4. Development of a biokinetic model describing N_2O production and liquid-gas transfers

The standard ASM2d (Henze et al., 2000), calibrated and validated by Zaborowska et al. (2017), was used as a core model and was extended in the present study with the additional processes, specifically related to N_2O:

- N_2O production/consumption,
- Transformations of N compounds (NO_3^--N to NO_2^--N) by DPAOs,
- Air-stripped N_2O emissions and saturation-induced liquid-gas transfers for N_2O.

These extensions were integrated into the new ASM2d-N_2O model. Two N_2O production pathways by AOB and N_2O production and consumption by denitrifying ordinary heterotrophic organisms (OHOs) were incorporated into the model following the concept of Lu et al. (2018). DPAOs were assumed to reduce NO_3^--N only to NO_2^--N following the concept of Wisniewski et al. (2018). The air-stripped N_2O emissions and saturation-induced liquid-gas transfers for N_2O were introduced into the model by adding a new state variable. The N_2O emission rates in the anoxic and aerobic zones were calculated based on mathematical models (Baresel et al., 2016; Marques et al., 2016) that described the N_2O liquid-gas transfers and the air-stripping processes (Equations (S1)-(S5)). Further details regarding the model development can be found in the SI, including the definitions of the state variables, stoichiometric matrices and process rate equations (Tables S3-S9). A full list of the model parameters in the ASM2d-N_2O can be found in Table S14.

2.5. Calibration and validation of the biokinetic model

To reduce the model uncertainty and minimize the number of the adjusted parameters, Domingo-Félez et al. (2017) proposed a three-step procedure (model calibration, recalibration and validation). In the present study, a similar approach was adopted (with details shown in Figure 2):

(i) Model calibration without consideration of the N_2O data (trial no.1, laboratory-scale and full-scale), focusing on the principal biochemical processes (nitrification, denitrification, P release/uptake),

(ii) Model recalibration with consideration of the N_2O data (trial no. 2, laboratory-scale), focusing on the liquid N_2O production,

(iii) Model validation with consideration of the N_2O data (trial no. 2, full-scale), focusing on the liquid N_2O production and gaseous N_2O emissions.

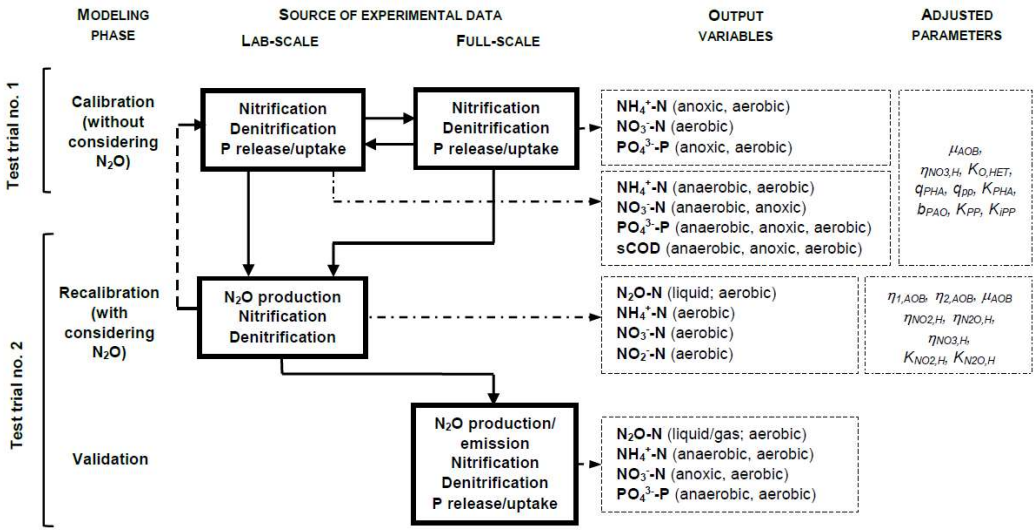

Figure 2. The model calibration and validation procedure developed specifically for the studied plant based on the available data

A sensitivity analysis identified the relative importance of different model parameters on the model outputs (NH_4^+-N, NO_2^--N, NO_3^--N, PO_4^{3-}-P, sCOD and N_2O-N). A one-variable-at-a-time sensitivity analysis was applied using a special GPS-X 7.0 (Hydromantis/Canada) utility called the "Phase dynamic" sensitivity analyser, and a relative uncertainty of 20% (specifically, ±10% of the adjusted value) was assigned to each model parameter (Equation (S6)). The parameter estimation was performed using a GPS-X utility called "Optimizer" using the Nelder-Mead simplex method with the maximum likelihood objective function.

The average values from the dynamic simulations were compared with steady-state predictions to evaluate the accuracy of steady-state predictions and their applicability in the model-based analysis of strategies for mitigation of N_2O production.

2.6. Model-based evaluation of N_2O production and emission

Strategies for the mitigation of N_2O production at the studied WWTP were analysed with the validated model by changing input variables, such as the DO concentration in the aerated zones and the MLR ratio. The aim of the analysis was to investigate the interactions between N_2O production and emissions, TN removal efficiencies, and energy consumption. The DO concentrations and MLR ratios were selected as examples of the most influential manipulated variables affecting WWTP performance. These variables were investigated in several previous theoretical simulation studies to quantify GHG emissions at different control strategies (Flores-Alsina et al., 2011; Kim et al., 2015; Massara et al., 2018; Mikosz, 2016; Sweetapple et al., 2014) and in a laboratory-scale reactor (Yan et al., 2016).

A series of steady-state simulations were conducted for a wide range of the two variables, i.e., 0.1-3.5 mg O_2/L (with a step of 0.1 mg O_2/L) for the DO concentration and 340-1000% (with a step of 30%) of the influent flowrates for the MLR ratio. The steady-state simulations (252 runs) were conducted automatically using the "Analyze" tool in GPS-X. The 3-D graphs were developed in the Surfer software (Golden Software LLC./USA) and the kriging method was used for interpolation of the data. Based on the results of all 252 runs, the optimal points (minima) were searched with respect to N_2O emissions from the specific compartments and

the minimal carbon footprint for the entire bioreactor. The average operational parameters and wastewater characteristics for the summer of 2016 (Table S2 in the SI) were used to obtain results at the reference state.

The considered total energy demand comprised the energy related to the manipulated variables, i.e., electric energy for aeration and MLR pumping. The power consumption by the fine bubble diffused aeration system was calculated based on the physical characteristics of the aeration system and the volumetric air flowrate imposed by the DO control system (Table S10 in the SI). Equations (S7)-(S10) were used to calculate the wire power consumption by the blowers and by the MLR pumps. The dynamic predictions of wire power consumption by the blowers were validated using the data from electricity meters in the full-scale measurement campaign.

2.7. Evaluation of the carbon footprint

The carbon footprint was expressed in CO_2 equivalents (CO_{2e}) with respect to direct emissions (related to the biochemical processes in the bioreactor) and indirect emissions (related to the electricity consumption in the processes). The considered total carbon footprint was composed of the CO_{2e} related to N_2O emissions from the specific compartments (anaerobic, anoxic and aerobic) of the bioreactor, and the overall energy demand for aeration and MLR pumping. The direct CO_{2e} emissions were calculated by multiplying the predicted fluxes of gaseous N_2O emitted from the bioreactor by GWP = 265 CO_{2e} (IPCC, 2014). Predictions of the aeration and pumping wire power (in kW) were multiplied by the time period under consideration to obtain the daily energy consumption (in kWh). It was assumed that electricity was imported to the

studied WWTP from the external grid. Thus, the indirect CO_{2e} emissions were calculated by multiplying the electricity consumption by the default amount of CO_2 (0.8 kg CO_2/kWh) that was emitted during electricity generation by the industrial power plants in Poland (KOBiZE, 2017).

3. Results and discussion

3.1. Model calibration without consideration of N_2O data (trial no. 1, laboratory-scale and full-scale)

The iterative model calibration, without consideration of the N_2O data, was based on the results of the laboratory experiments in trial no.1 (NH_4^+-N, NO_3^--N, PO_4^{3-}-P and sCOD). Model predictions were first fitted to the measured data by adjusting the key parameter values for the P uptake and release (q_{PHA}, q_{pp} and K_{PHA}), denitrification ($\eta_{NO3,H}$) and nitrification (μ_{AOB}). However, further modifications ($K_{O,HET}$, b_{PAO}, K_{PP} and K_{iPP}) were needed to improve the fit of the observed concentrations (NH_4^+-N, NO_3^--N and PO_4^{3-}-P) in the full-scale test in trial no. 1. The model predictions and measured data from the laboratory-scale ($r \geq 0.94$) and full-scale ($r \geq 0.67$) tests are presented in Figures S2-S3 (SI). Regarding the laboratory-scale experiments, the model predictions of ASM2d-N_2O (this study) and ASM2d (Zaborowska et al., 2017) were consistent ($R^2 \geq 0.92$), as shown in Figure S2 (d-g) and Table S11 (SI). Regarding the full-scale campaign, the model predictions of ASM2d-N_2O and ASM2d (Figure S3d-f) were also consistent ($R^2 \geq 0.65$). For PO_4^{3-}-P and NO_3^--N, the predictions even improved in the present study in comparison with the previous study (Zaborowska et al., 2017) (Table S12).

3.2. Model recalibration with consideration of N_2O data (trial no. 2, laboratory-scale)

Model recalibration with consideration of the N_2O data was based on the results of the laboratory experiments in trial no. 2 (liquid N_2O production). The model predictions were fitted to the measured data first by adjusting only the parameters sensitive to N_2O and not directly affecting the four target variables in the first-step calibration, i.e., the additional key parameters for the N_2O production by both AOB ($\eta_{1,AOB}$ and $\eta_{2,AOB}$) and heterotrophic denitrifiers ($\eta_{NO2,H}$, $\eta_{N2O,H}$, $K_{NO2,H}$ and $K_{N2O,H}$). The parameters most sensitive to N_2O ($\eta_{NO3,H}$ and μ_{AOB}), which were obtained from the first-step calibration, were also taken into account during the recalibration. A list of all adjusted parameters along with their sensitivities is presented in Table S13 and further discussed in the SI. Among the sensitive parameters adjusted in the present study, the parameters for N_2O production and consumption pathways were consistent with the literature values, apart from the nitrite reduction factor for heterotrophs ($\eta_{NO2,H}$). The adjusted $\eta_{NO2,H}$ = 0.60 mg N/L was higher than the literature values ($\eta_{NO2,H}$ = 0.35 mg N/L) (Lu et al., 2018), which indicated the predominance of heterotrophic denitrification pathway. The remaining parameters were adopted from ASM2d (24 ASM2d defaults and 12 from Zaborowska et al. (2017)) and additionally from literature (the N_2O production/consumption, the transformations of N compounds (NO_3^--N to NO_2^--N) by DPAO, the air-stripped N_2O emissions and the saturation-induced liquid-gas transfers for N_2O) (Table S14). The values of these parameters were generally close to the ASM2d defaults or within the ranges reported in the literature.

The model predictions and measured data of the laboratory-scale tests are presented in Figure 3 ($r \geq 0.94$). In both experiments, the presence of DO induced nitrification leading to NO_3^--N accumulation, while NO_2^--N levels remained significantly lower (< 0.6 mg N/L) (Figures 3a and 3d). During the aerobic test at DO = 0.5 mg O_2/L (Figure 3a-c), the highest liquid N_2O concentrations (0.06 mg N/L) were observed after 2 h of the reaction phase (Figure 3b). The simulation results suggested that heterotrophic denitrification made a significantly higher contribution to the N_2O production in comparison with the NH_2OH oxidation pathway (when excluding the simultaneous N_2O consumption by heterotrophs) (Figure 3c), whereas the estimated contribution from autotrophic denitrification was negligible in that experiment. The dominant contribution of the heterotrophic pathway could be attributed to the predominant abundance of heterotrophs over nitrifiers in the studied system. In the experiment at DO = 1.0 mg O_2/L (Figure 3d-f), a two-fold lower liquid N_2O concentration (0.03 mg N/L) was observed (Figure 3e), partially due to higher aeration intensities resulting in a stronger N_2O stripping effect (0.018 g N/d at DO = 1.0 mg O_2/L vs 0.003 g N/d at DO = 0.5 mg O_2/L). At the higher DO concentration, the anoxic activity of heterotrophs was significantly inhibited and the estimated contributions of heterotrophic denitrification and of the NH_2OH oxidation pathways became comparable in terms of N_2O production (when excluding the simultaneous N_2O consumption by heterotrophs). The autotrophic denitrification pathway was once again marginal (Figure 3f). In the present study, the adjusted oxygen half-saturation coefficient ($K_{O,H}$) was within the range presented in the literature (0.01-0.5 mg O_2/L) (Mannina et al., 2012). By changing $K_{O,H}$ from 0.13 (Domingo-Félez et al., 2017) to 0.3 (this study), the estimated anoxic activity of denitrifying heterotrophs approximately doubled for the actual

aerobic conditions (DO = 1.0 mg O_2/L). These results suggest that N_2O may be explicitly produced by both AOB (NH_2OH oxidation) and heterotrophic denitrifiers. It should also be emphasized that the simultaneous N_2O consumption by heterotrophs significantly reduced their net contribution to N_2O accumulation (Figures 3c and 3f).

Various dominant pathways of N_2O production and emissions under aerobic conditions have been reported in other studies. Tallec et al. (2008) found that below 0.3 mg O_2/L, heterotrophic denitrification was the major process responsible for N_2O emissions in a denitrifying AS system. However, the authors suggested that in the DO range of 0.4 to 1.1 mg O_2/L, N_2O production resulted from two processes, including autotrophic (60%) and heterotrophic (40%) denitrification. Shen et al. (2015) demonstrated that heterotrophic activities significantly affected N_2O emission during nitrification. In recent studies, heterotrophic denitrifiers were found to be the key contributors to N_2O production in AS under aerobic conditions (DO = 0.2-6.5 mg O_2/L) at low C/N ratios (Domingo-Félez et al., 2017), whereas the predominance of the NH_2OH pathway was shown for either low or very high NO_2^--N concentrations (e.g. < 3.5 and 700-1120 mg N/L) and DO concentrations from 0.5 to 2.0 mg O_2/L (Ni et al., 2014). AOB were identified as the major N_2O producers by Guo (2014), however assuming considerable consumption of N_2O by heterotrophs (the net N_2O production by heterotrophs).

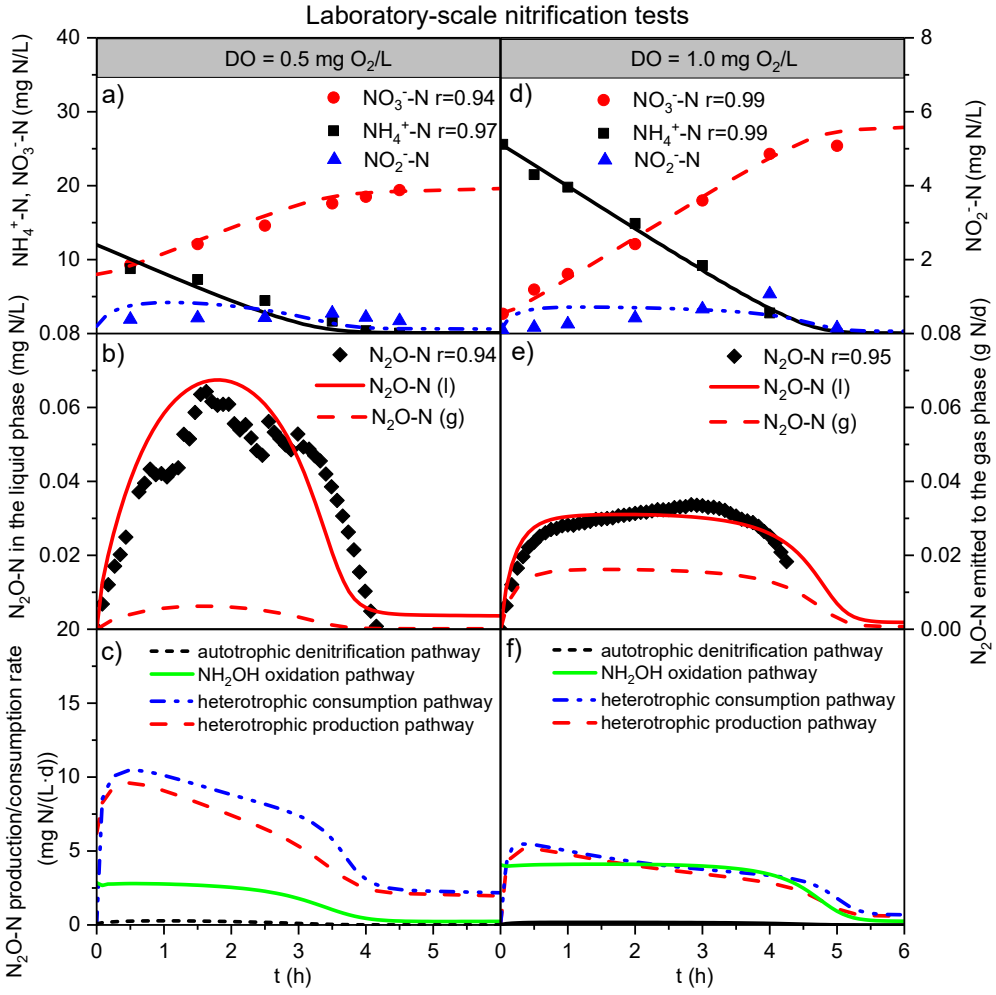

Figure 3. Model predictions (lines) vs. measured data (scatters) of the N compounds (NO_3^--N, NH_4^+-N, NO_2^--N, and N_2O (liquid (l), gas (g)) for the laboratory-scale nitrification tests and the N_2O production/consumption rates for each pathway at DO = 0.5 mg O_2/L (a-c); DO = 1.0 mg O_2/L (d-f)

3.3. Model validation (trial no. 2, full-scale)

Model validation was performed based on the full-scale test in trial no. 2 (including liquid N_2O production and gaseous N_2O emissions). Figure 4 shows the dynamic output predictions and measurements in the full-scale bioreactor. The model accurately predicted the behaviour of the N compounds (NH_4^+-N and NO_3^--N) ($r \geq 0.83$) and PO_4^{3-}-P ($r \geq 0.64$) in both the anaerobic and

aerobic compartments of the bioreactor (Figure 4a-c). The diurnal variability in N_2O, emitted from the aerobic zones to the gas phase (Figure 4d), followed the diurnal trends of the NH_4^+-N and NO_3^--N concentrations. The predicted liquid N_2O concentrations revealed a smaller variability in comparison with the gaseous N_2O emissions (Figure 4e). The N_2O emissions coincided with the diurnal variations in NH_4^+-N, NO_2^--N and NO_3^--N concentrations (Figure S4). Daelman et al. (2015) also found that the N_2O emissions from a carrousel reactor coincided with the diurnal variations in NO_2^--N and NO_3^--N concentrations and NH_4^+-N loading rates. A conjunction between the maximum N_2O emissions and high NH_4^+-N concentrations was found in an aerobic compartment of the Ludzack-Ettinger process configuration operated at DO < 2.5 mg O_2/L (Guo, 2014).

In the full-scale bioreactor at the Slupsk WWTP, the NH_4^+-N concentrations in the aerobic compartments were low (2.1±1.2 mg N/L in AE1 and 0.2±0.1 mg N/L in AE2 effluent). The N_2O heterotrophic production rates in AE1 and AE2 (for DO = 2.25 ± 0.5 mg O_2/L) were reduced by 96% and 98%, respectively, in comparison with the rates in AO1 due to DO inhibition and carbon substrate limitation. The contribution from NH_2OH oxidation was significant in AE1/2, but was still lower than the heterotrophic denitrification pathway (72% in AE1 and 81% in AE2). Despite the predominance of different N_2O production pathways, the results of the present study are consistent with the results of previous studies (Massara et al., 2018; Ni et al., 2015; Peng et al., 2014; Pocquet et al., 2016) demonstrating that the NH_2OH oxidation and autotrophic denitrification pathways were enhanced, when increasing and decreasing, respectively, the DO concentrations.

A comparison between the mean values predicted from the dynamic simulations, the steady-state predictions and the measurements for the second full-scale campaign is shown in Table S15 (SI). Both dynamic predictions (mean values) and steady-state predictions were consistent and comparable with the measured data (the relative differences ranged from 0 to 8.2%). Therefore, it was shown that steady-state predictions could be reliable and useful for the analysis of strategies for mitigating N_2O production in the full-scale bioreactor (section 3.5) and for decreasing the carbon footprint of the studied plant (section 3.6).

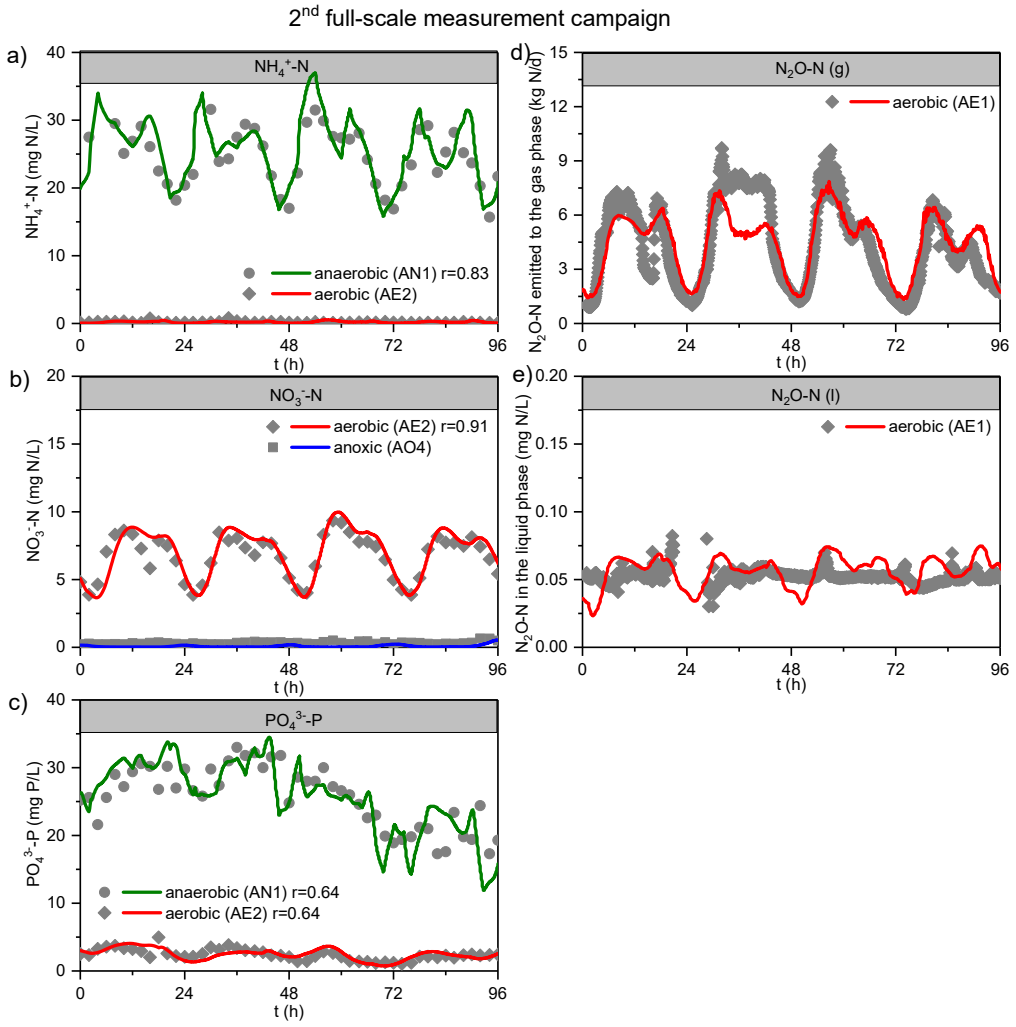

Figure 4. Model predictions (solid lines) vs. measured data (scatters) from the second full-scale measurement campaign: (a) NH_4^+-N in the first anaerobic (AN1) and last aerobic (AE2) compartments; (b) NO_3^--N in the last anoxic (AO4) and last aerobic (AE2) compartments; (c) PO_4^{3-}-P in the first anaerobic (AN1) and last aerobic (AE2) compartments; (d) the load of gaseous N_2O-N emitted in the first aerobic (AE1) compartment; (e) liquid N_2O-N concentrations in the first aerobic (AE1) compartment

3.4. Advantages and novelty of the model developed in this study

In comparison with previous full-scale N_2O modelling studies (limited to N removal systems without EBPR), the present model revealed some important advantages and novel aspects. The results presented in the previous studies showed discrepancies between the measured data and model predictions. In the benchmark simulation model incorporating GHG (BSM2G), Arnell et al. (2017) considered only nitrogen N transformation and N_2O production via the autotrophic denitrification pathway. The results showed that the average levels of the modelled emissions were in agreement with the measured values. However, the full dynamics of the measured emissions were not well-predicted by the model. The extended ASM3 model presented by Blomberg et al. (2018) was able to capture the dynamics of the liquid-phase N_2O transfer in the aeration tank. However, the model could predict only the variations in N_2O emissions, while the base levels of the modelled values were notably higher when compared to the measured emissions. The discrepancies were partially attributed to the imperfections in the models describing the N_2O stripping effect. An oxidation ditch and an SBR plant were investigated by Ni et al. (2013). Although N_2O production from autotrophic denitrification was not considered

in that model, good agreement was found between model simulations and measured N_2O levels, as well as with other N compounds, possibly due to predomination of the NH_2OH oxidation pathway. A study on a step-feed bioreactor (Ni et al., 2015) is an example of implementation and validation of a multi-pathway N_2O model in a full-scale N removal system dominated by AOB-mediated transformations. Those results showed the importance of a comprehensive approach to correctly identify the N_2O production pathways and accurately predict N_2O behaviour.

The novelty of the model in the present study lies in the description of all N_2O production pathways in the combined N and P removal system and evaluation of the integrated model against the full-scale experimental data from such a system. The model covers all known aspects related to N_2O behaviour in BNR WWTPs, including the three known pathways of N_2O production in N transformations, the role of DPAO in denitrification, and N_2O liquid-gas transfer. The model was successfully calibrated and validated with respect to the behaviour of N_2O and other important state variables (NO_3^--N, NH_4^+-N and PO_4^{3-}-P) both in the full-scale BNR bioreactor and in the laboratory experiments focused on specific biochemical processes. Maximization of the available data for the plant was proven to be an effective approach to constrain the effort made for extending the standardized models to include the module describing N_2O. The validated model can thus become a tool for developing N_2O mitigation strategies and for carbon footprint analysis.

3.5. Analysis of strategies for mitigation of N_2O production.

Figures 5a-b show the combined effects of the DO concentrations in the aerobic zones and the MLR on N_2O production in the AE1 and AE2 compartments, respectively. The predicted total N_2O emission rates from the bioreactor are shown in Figure 5c. The reference state represents the current operational conditions (DO = 2.5 mg O_2/L, MLR = 500%) and the average wastewater characteristics in the summer period. Within the analysed ranges, the liquid N_2O predictions in AE2 were generally independent of the MLR ratios (N_2O decreasing with increasing DO), whereas the minimum N_2O value in AE1 (< 0.05 mg N/L) was obtained at the region close to MLR = 600% and DO = 3.5 mg O_2/L (Figure 5a-b). A sudden accumulation of N_2O was observed in both AE1 and AE2 under DO limiting conditions (< 1.0 mg O_2/L) which reduced the efficiency of nitrification and favoured the anoxic activity of heterotrophs. A peak N_2O concentration in the liquid phase (0.27 mg N/L) was found in AE2 at DO = 0.4 mg O_2/L. Under these conditions, partial nitrification (nitritation) was favoured at the highest NO_2^--N concentrations (2.1 mg N/L). In both aerobic compartments at DO < 0.3 mg O_2/L, AOB and NOB activities suddenly dropped and subsequent production of NO_2^--N, NO_3^--N and N_2O was severely restrained. Similar relationships were found in other simulation studies investigating models of a modified Ludzack-Ettinger (MLE) configuration (Mikosz, 2016) and of an A_2O bioreactor (Massara et al., 2018). The increased N_2O production via nitrification inhibition and NO_2^--N accumulation under DO concentrations <1.5 mg O_2/L was also demonstrated by Ni et al. (2011) and Peng et al. (2014). The similarity of the literature data to results obtained in this study may suggest that DPAOs do not play a significant role in N_2O production in combined N and P removal systems.

The increase in the N_2O concentrations in AE1, observed at MLR > 800% and DO > 2 mg O_2/L, was significantly lower in comparison with the accumulation at DO < 1 mg O_2/L. However, these results are still important due to the combined influence of DO and MLR on N_2O in both aerobic and anoxic compartments and further influence on the total carbon footprint of the bioreactor (Figure 6a). In fact, the accumulation of NO_3^--N and denitrification intermediates (NO_2^--N and N_2O) can occur for different MLRs depending on the local conditions, e.g., process configuration, mixing conditions and influent characteristics (COD/N ratio). For example, Yan et al. (2016) observed a similar phenomenon with MLR increasing from 100% to 300% in a laboratory-scale A_2O reactor operated at DO = 2 mg O_2/L in the aerobic compartment. That behaviour was also attributed to the increased concentrations of NO_3^--N and DO transferred to the anoxic zone. However, a low influent ratio of COD/NH_4^+-N = 4.5 resulted in poor TN removal rates (46-62%) and enhanced N_2O production at lower MLR ratios in comparison with the present study (influent COD/NH_4^+-N = 16; TN removal = 90%).

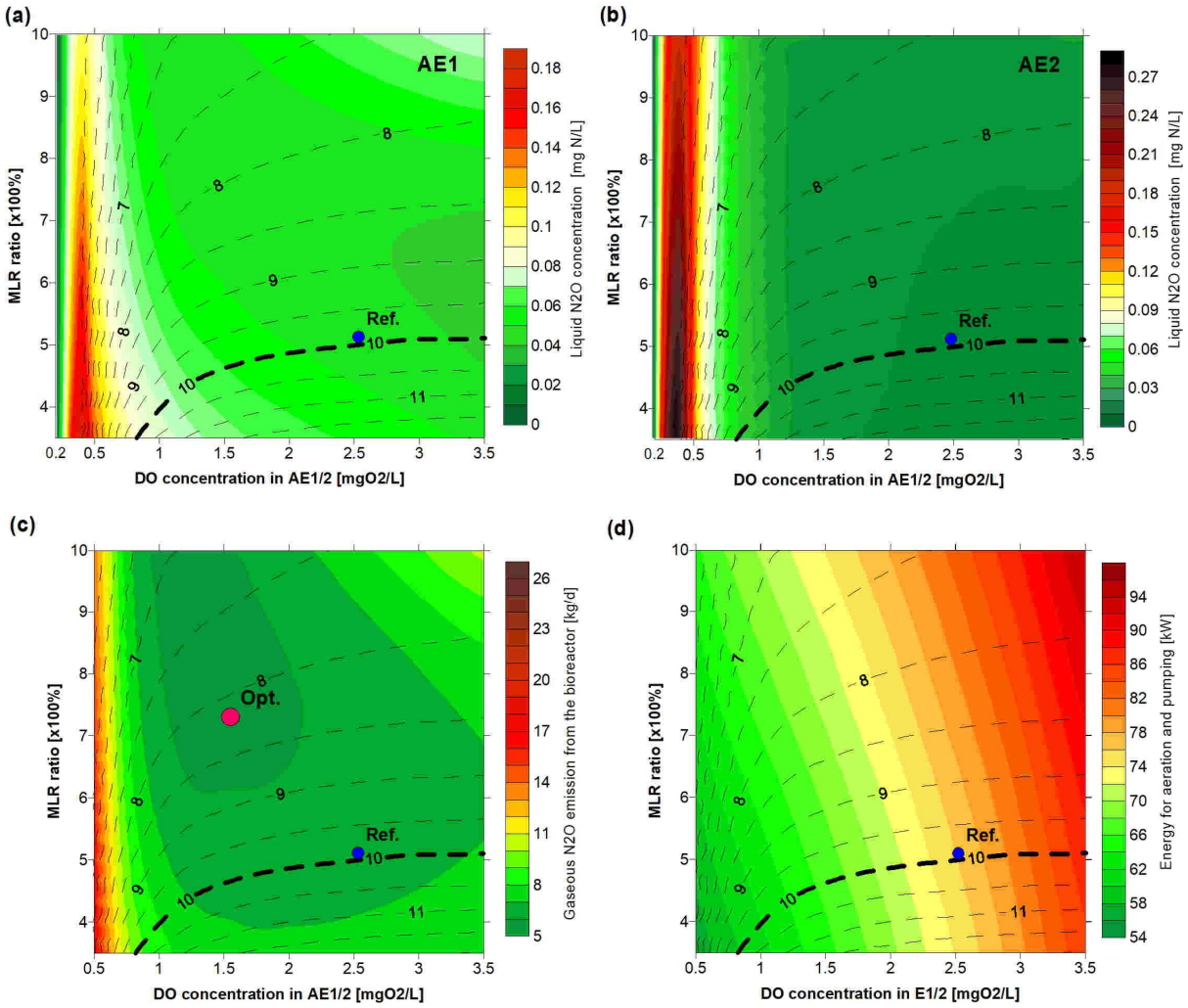

Figure 5. Predicted effluent TN concentrations (mg N/L) (dashed lines) and liquid N_2O concentrations in AE1 (colour scale) (a); liquid N_2O concentrations in AE2 (colour scale) (b); gaseous N_2O emission rates from the bioreactor (colour scale) (c); energy consumption for aeration and pumping (colour scale) (d); ("Ref."- the reference state, "Opt."- the optimal state)

Regarding the gaseous N_2O emissions from the studied bioreactor, the aerated compartments were the dominant contributors primarily due to the air stripping effect. In the anoxic zone, most of the produced N_2O was simultaneously consumed in heterotrophic denitrification. Within the range of the investigated DO and MLRs, the anoxic zone contributed only to 0.8-

11% of the total gaseous N_2O emissions from the bioreactor. For comparison, a low contribution from the anoxic zones (1.5%) was observed in a full-scale WWTP employing the AS process (Blomberg et al., 2018). In contrast, in a laboratory-scale A_2O configuration, the anoxic section contributed to over 20% of the total N_2O emissions (Yan et al., 2016), possibly due to the relatively high N_2O concentration in that section and intensive stirring. It should be emphasized that the effects of stirring are not taken into consideration in the equation describing N_2O liquid-gas transfers in anoxic zones (Equation (S3) in the SI).

The emission rates from the studied aerobic zone were affected by both liquid N_2O concentrations in AE1/2 and by air flowrate (stripping). The operational strategy of maintaining DO = 1-2 mg O_2/L in the aerobic zones and increasing the MLR ratio (> 500%) resulted in lower N_2O emissions. The optimal state (represented by the "Opt." point) referred to the following set points: DO = 1.5 mg O_2/L and MLR = 730% (Figure 5c). At that state, the lowest N_2O emissions from the bioreactor were predicted (5.8 kg/d) without compromising the effluent TN limit of 10 mg N/L. When applying the optimal DO and MLR set points under the dynamic conditions of the full-scale measurement campaign (trial no.2), the predicted mean N_2O emission was 5.9±2.0 kg/d (vs. 5.6 kg/d under the steady-state conditions).

The modification of the operational variables affected the energy balance of the studied plant. Figure 5d shows that the DO set point was more significant than MLR and determined the total energy consumption due to higher blower wire power in comparison to the pump wire power. The decreased aeration intensity resulted in lower energy consumption, but an excessive

reduction (DO < 1.0 mg O_2/L) significantly enhanced N_2O emissions. By increasing the MLR, the effluent TN concentrations decreased, but the energy consumption simultaneously increased. Reducing the DO concentration from 2.5 mg O_2/L to 1.5 mg O_2/L and increasing the MLR from 500% to 730% resulted in decrease in the total energy demand by 7.4% (calculated based on the assumptions given in Section 2.6). This positive effect was obtained as the energy savings for aeration exceeded the increased energy consumption for MLR pumping. This aspect is further discussed with respect to the total carbon footprint of the studied bioreactor.

3.6. Carbon footprint analysis

Predicted CO_{2e} emissions under varying DO concentrations and MLR are shown in Figure 6a. At the reference state, the GHG emissions from the bioreactor reached 3.2 Mg CO_{2e}/d, but this value can be reduced by applying the proposed strategies for mitigation of N_2O production. The DO concentrations in the aerated zones were found to be the most significant factors affecting total GHG emissions, taking advantage of the synergy between the reduction in gaseous N_2O emissions and energy consumption. At the optimal state for the carbon footprint (DO = 1.3 mg O_2/L, MLR = 730%), the predicted energy consumption was reduced by approximately 9.5% in comparison with the reference state. Following the energy savings and reduction in N_2O emissions, the total carbon footprint was decreased by 10.3%. Regarding the potential reduction in the carbon footprint and the operational cost, the simulation results suggest that the studied WWTP can achieve better performance by applying reasonable measures. With respect to the relative energy savings, the results of the present study are

consistent with the findings of the theoretical modelling studies (Table S16 in the SI). The potential reductions in GHG emissions found in this study and in the literature emphasize the significance of either indirect or direct CO_{2e} emissions. Their contributions to the total carbon footprint can substantially differ among the plants. Moreover, the relative benefits to the GHG emissions reduction are affected by the conditions assumed at the reference state. A contribution of the N_2O equivalent emissions to the total carbon footprint of the bioreactor is shown in Figure 6b. Within the range of analysed DO and MLRs, the share of N_2O was in the range 51-80%. For comparison, a contribution of 78% was reported for a full-scale BNR WWTP (Daelman et al., 2013). In an SBR plant, Rodriguez-Caballero et al. (2015) estimated that the contribution of N_2O emissions was in the range of 24-80% under different cycle configurations. In contrast, Aboobakar et al. (2013) reported that N_2O emissions added only 13% to the carbon footprint associated with the energy requirements. Apart from specific plant configurations and operational conditions, these differences can also be attributed to the CO_{2e} emission factor related to the assumed energy source (renewable vs. non-renewable).

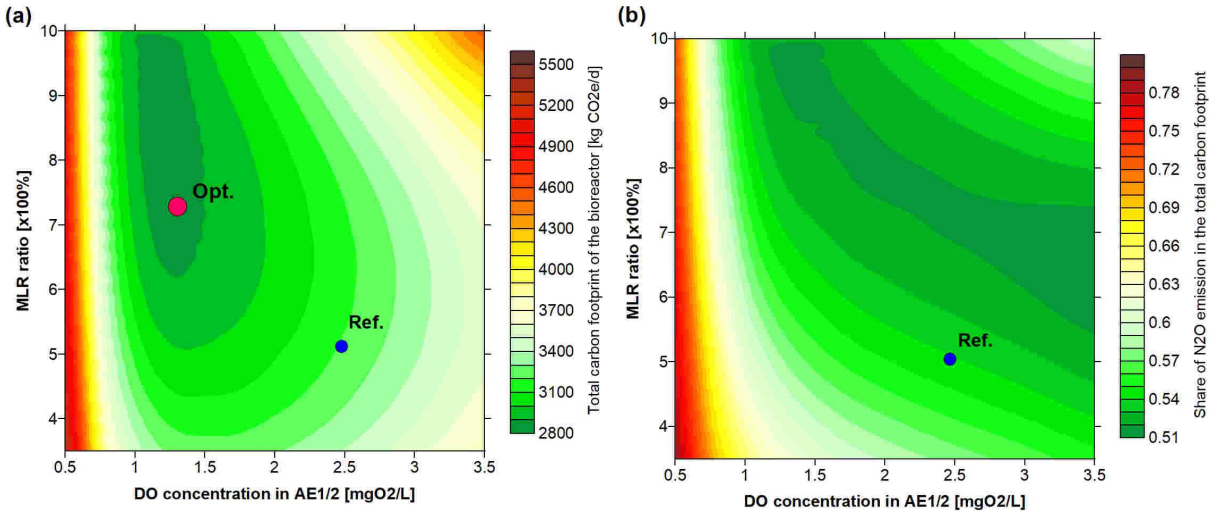

Figure 6. Predicted total carbon footprint of the bioreactor (a) and share of N_2O equivalent emissions in the total carbon footprint (b) ("Ref."- the reference state; "Opt."- the optimal state)

While mitigating N_2O emission and decreasing the carbon footprint, a potential trade-off with other objectives of plant performance, such as the effluent quality, needs to be considered. The simulation results revealed that at the optimal state with respect to the total carbon footprint, TN concentrations were 20% lower in comparison with the reference state. As a result of the proposed strategy, an increasing trend in the effluent liquid N_2O concentrations was observed. However, the predicted value (0.026 mg N/L) was as low as 0.3% of the effluent TN concentration at the optimal state. It should also be noted that N_2O has a relatively high solubility in water and accumulations of N_2O in the liquid phase may not directly result in emissions to the atmosphere. The overall environmental impact (including the eutrophication potential) remains out of the scope of the present study but could be part of a life cycle analysis as an extension of the carbon footprint analysis.

4. Conclusions

- The model developed and validated in this study could be a useful tool for analysing the multivariable problem of mitigation of N_2O production in combined N-P activated sludge systems. To minimize N_2O production in a full-scale bioreactor, without compromising the effluent TN standards, the DO concentrations in the aerobic zone should be decreased and maintained at 1-2 mg O_2/L and the MLR should exceed 500% of the influent flowrate. The lower energy consumption for aeration would result in an energy credit exceeding the higher energy consumption for pumping.
- In the validation phase, heterotrophic denitrification was found to be the main pathway of N_2O production under both anoxic (99%) and aerobic conditions (72-81%), when excluding the simultaneous N_2O consumption by heterotrophic denitrifiers. This behaviour could primarily be attributed to the predominant abundance of heterotrophic denitrifiers over AOB, even though the estimated denitrification rates under aerobic conditions were reduced by 94-98% in comparison with the anoxic rates.
- Within the range of manipulated DO and MLRs, N_2O emissions from the bioreactor were responsible for over 50% of the total carbon footprint despite a high CO_{2e} emission factor related to the non-renewable energy source used in the external power plant. The potential reduction in the total carbon footprint was estimated at 10% in comparison with the current operational conditions by applying the recommended strategy of reducing DO concentrations and enhancing MLR ratios for mitigating N_2O production and emissions. These results suggest that considerable improvements with respect to the carbon footprint of BNR WWTPs can be achieved without substantial upgrades and increased costs.

Acknowledgements

This work was financially supported from Polish-German Cooperation for Sustainable Development Programme operated by the National Centre for Research and Development, project no. WPN/7/2013 "Reduction of N_2O emissions from wastewater treatment plants - measurements, modelling and process optimization" (RENEMO).

Appendix A. Supporting Information

Supporting information contains the proposed procedure, routine operational data, details related to the analytical methods, model development, definition of the state variables, stoichiometric matrices, kinetic rate equations, model parameters, sensitivity analysis and further modelling results.

References

Aboobakar, A., Cartmell, E., Stephenson, T., Jones, M., Vale, P., Dotro, G., 2013. Nitrous oxide emissions and dissolved oxygen profiling in a full-scale nitrifying activated sludge treatment plant. Water Res., 47, 524–534. DOI: 10.1016/j.watres.2012.10.004.

Arnell M., Rahmberg M., Oliveira F., Jeppsson U., 2017. Multi-objective performance assessment of wastewater treatment plants combining plant-wide process models and life cycle assessment. J. Water and Climate Change, 08(4), 715-729; DOI: doi.org/10.2166/wcc.2017.179.

Baresel, C., Andersson, S., Yang, J., Andersen, M.H., 2016. Comparison of nitrous oxide (N_2O) emissions calculations at a Swedish wastewater treatment plant based on water concentrations versus off-gas concentrations. Adv. Clim. Change Res., 7, 185–191. DOI: 10.1016/j.accre.2016.09.001.

Blomberg, K., Kosse, P., Mikola, A., Kuokkanen, A., Fred, T., Heinonen, M., Mulas, M., Lübken, M., Wichern, M., Vahala, R., 2018. Development of an extended ASM3 model for predicting the nitrous oxide emissions in a full-scale wastewater treatment plant. Environ. Sci. Technol., 52, 5803-5811; DOI: 10.1021/acs.est.8b00386.

Campos, J.L., Valenzuela-Heredia, D., Pedrouso, A., Val Del Río, A., Belmonte, M., Mosquera-Corral, A., 2016. Greenhouse Gases Emissions from Wastewater Treatment Plants: Minimization, Treatment, and Prevention. J. Chem., vol. 2016, 1-12; DOI: 10.1155/2016/3796352.

Chen, Y., Wang, D., Zheng, X., Li, X., Feng, L. & Chen, H., 2014. Biological nutrient removal with low nitrous oxide generation by cancelling the anaerobic phase and extending the idle phase in a sequencing batch reactor. Chemosphere 109, 56–63. http://dx.doi.org/10.1016/j.chemosphere.2014.02.011.

Daelman, M.R.J., van Voorthuizen, E.M., van Dongen, L.G.J.M., Volcke, E.I.P., van Loosdrecht, M.C.M., 2013. Methane and nitrous oxide emissions from municipal wastewater treatment: results from a long-term study. Water Sci. Technol., 67 (10), 2350-2355; DOI: 10.2166/wst.2013.109.

Daelman, M.R.J., van Voorthuizen, E.M., van Dongen, U.G.J.M., Volcke, E.I.P., van Loosdrecht, M.C.M., 2015. Seasonal and diurnal variability of N_2O emissions from a full-

scale municipal wastewater treatment plant. Sci. Total Environ., 536, 1–11; DOI: 10.1016/j.scitotenv.2015.06.122.

Domingo-Félez, C., Pellicer-Nàcher, C., Petersen, M.S., Jensen, M.M., Plósz, B.G., Smets, B.F., 2017. Heterotrophs are key contributors to nitrous oxide production in activated sludge under low C-to-N ratios during nitrification-Batch experiments and modeling. Biotechnol. Bioeng., 114, 132–140; DOI: 10.1002/bit.26062.

Flores-Alsina, X., Corominas, L., Snip, L., Vanrolleghem, P.A., 2011. Including greenhouse gas emissions during benchmarking of wastewater treatment plant control strategies. Water Res., 45, 4700-4710. DOI: 10.1016/j.watres.2011.04.040.

Guo, L.S., 2014. Greenhouse gas emissions from and storm impacts on wastewater treatment plants: Process modelling and control. PhD thesis. Laval University, Canada.

de Haas, D., Hartley, K., 2004. Greenhouse gas emission from BNR plants: do we have the right focus? In: Proceedings of EPA Workshop: Sewage Management: Risk Assessment and Triple Bottom Line, 5–7 April 2004, Cairns, Australia.

Henze, M., Gujer, W., Mino, T., van Loosdrecht, M.C.M., 2000. Activated Sludge Models ASM1, ASM2, ASM2d and ASM3. IWA Publ., London.

IPCC, 2014. Intergovernmental Panel on Climate Change Fifth Assessment Report. https://www.ipcc.ch/assessment-report/ar5/

Kim, D., Bowen, J.D., Ozelkan, E.C., 2015. Optimization of wastewater treatment plant operation for greenhouse gas mitigation. Journal of Environmental Management, 163, 39-48. DOI: 10.1016/j.jenvman.2015.07.005.

KOBiZE, 2017. Emission factors of CO_2, SO_2, NO_x, CO and total dust for electric energy, on the basis of information contained in the National Database on greenhouse gas emissions and other substances for 2016. National Center for Emission Management (KOBiZE), Warsaw/Poland (*in Polish*).

Liu, Y., Peng, L., Chen, X., Ni, B.-J., 2015. Mathematical Modeling of Nitrous Oxide Production during Denitrifying Phosphorus Removal Process. Environ. Sci. Technol., 49, 8595-8601. DOI: 10.1021/acs.est.5b01650.

Lu, X., D. S. Pereira, T., Al-Hazmi, H.E., Majtacz, J., Zhou, Q., Xie, L., Makinia, J., 2018. Model-Based Evaluation of N_2O Production Pathways in the Anammox-Enriched Granular Sludge Cultivated in a Sequencing Batch Reactor. Environ. Sci. Technol., 52, 2800–2809; DOI: 10.1021/acs.est.7b05611.

Mannina, G., Cosenza, A., Viviani, G., 2012. Uncertainty assessment of a model for biological nitrogen and phosphorus removal: Application to a large wastewater treatment plant. Phys. Chem. Earth Parts ABC 42–44, 61–69. https://doi.org/10.1016/j.pce.2011.04.008

Mannina, G., Capodici, M., Cosenza, A., Di Trapani, D., van Loosdrecht, M.C.M., 2017. Nitrous oxide emission in a University of Cape Town membrane bioreactor: The effect of carbon to nitrogen ratio. J. Clean. Prod., 149, 180–190; DOI: 10.1016/j.jclepro.2017.02.089.

Marques, R., Rodriguez-Caballero, A., Oehmen, A., Pijuan, M., 2016. Assessment of online monitoring strategies for measuring N_2O emissions from full-scale wastewater treatment systems. Water Res., 99, 171–179; DOI: 10.1016/j.watres.2016.04.052.

Massara, T.M., Malamis, S., Guisasola, A., Baeza, J.A., Noutsopoulos, C., Katsou, E., 2017. A review on nitrous oxide (N2O) emissions during biological nutrient removal from municipal wastewater and sludge reject water. Sci. Total Environ., 596–597, 106–123; DOI: 10.1016/j.scitotenv.2017.03.191.

Massara, T.M., Solís, B., Guisasola, A., Katsou, E., Baeza, J.A., 2018. Development of an ASM2d-N_2O model to describe nitrous oxide emissions in municipal WWTPs under dynamic conditions. Chem. Eng. J., 335, 185–196; DOI: 10.1016/j.cej.2017.10.119.

Mikosz, J., 2016. Analysis of greenhouse gas emissions and the energy balance in a model municipal wastewater treatment plant. Desalination Water Treat., 57, 28551–28559; DOI: 10.1080/19443994.2016.1192491.

Ni, B.-J., Pan, Y., van den Akker, B., Ye, L., Yuan, Z., 2015. Full-Scale Modeling Explaining Large Spatial Variations of Nitrous Oxide Fluxes in a Step-Feed Plug-Flow Wastewater Treatment Reactor. Environ. Sci. Technol., 49, 9176–9184; DOI: 10.1021/acs.est.5b02038.

Ni, B.-J, Peng, L., Law, Y., Guo, J., Yuan, Z., 2014. Modeling of nitrous oxide production by autotrophic ammonia-oxidizing bacteria with multiple production pathways, Environ. Sci. Technol., 48(7), 3916–3924; DOI: 10.1021/es405592h.

Ni, B.-J., Ruscalleda, M., Pellicer-Nàcher, C., Smets, B.F., 2011. Modeling Nitrous Oxide Production during Biological Nitrogen Removal via Nitrification and Denitrification: Extensions to the General ASM Models. Environ. Sci. Technol., 45, 7768–7776; DOI: 10.1021/es201489n.

Ni, B.-J., Ye, L., Law, Y., Byers, C., Yuan, Z., 2013. Mathematical modeling of nitrous oxide (N_2O) emissions from full-scale wastewater treatment plants. Environ. Sci. Technol., 47, 7795–7803; DOI: 10.1021/es4005398.

Ni, B.-J., Yuan, Z., 2015. Recent advances in mathematical modeling of nitrous oxides emissions from wastewater treatment processes. Water Res., 87, 336–346; DOI: 10.1016/j.watres.2015.09.049.

Pan, Y., van den Akker, B., Ye, L., Ni, B.-J., Watts, S., Reid, K., Yuan, Z., 2016. Unravelling the spatial variation of nitrous oxide emissions from a step-feed plug-flow full scale wastewater treatment plant. Sci. Rep., 6:20792, 1-10; DOI: 10.1038/srep20792.

Peng, L., Ni, B.-J., Erler, D., Ye, L., Yuan, Z., 2014. The effect of dissolved oxygen on N_2O production by ammonia-oxidizing bacteria in an enriched nitrifying sludge. Water Res., 66, 12-21; DOI: 10.1016/j.watres.2014.08.009.

Pocquet, M., Wu, Z., Queinnec, I., Spérandio, M., 2016. A two pathway model for N2O emissions by ammonium oxidizing bacteria supported by the NO/N_2O variation. Water Res., 88, 948–959; DOI: 10.1016/j.watres.2015.11.029.

Rodriguez-Caballero, A., Aymerich, I., Marques, R., Poch, M., Pijuan, M., 2015. Minimizing N_2O emissions and carbon footprint on a full-scale activated sludge sequencing batch reactor. Water Res., 71, 1–10. DOI: 10.1016/j.watres.2014.12.032.

Rodriguez-Caballero, A., Aymerich, I., Poch, M., Pijuan, M., 2014. Evaluation of process conditions triggering emissions of green-house gases from a biological wastewater treatment system. Sci. Total Environ., 493, 384–391. https://doi.org/10.1016/j.scitotenv.2014.06.015.

Shen L., Guan Y., Wu G., 2015. Effect of heterotrophic activities on nitrous oxide emission during nitrification under different aeration rates. Desalin Water Treat, 55:821–827. https://doi.org/10.1080/19443994.2014.928793.

Sun, S., Bao, Z., Sun, D., 2015. Study on emission characteristics and reduction strategy of nitrous oxide during wastewater treatment by different processes. Environ Sci Pollut Res 22:4222–4229. DOI 10.1007/s11356-014-3654-5

Schreiber, F., Wunderlin, P., Udert, K.M., Wells, G.F., 2012. Nitric oxide and nitrous oxide turnover in natural and engineered microbial communities: biological pathways, chemical reactions, and novel technologies. Front. Microbiol. 3. https://doi.org/10.3389/fmicb.2012.00372

Sweetapple, C., Fu, G., Butler, D., 2014. Multi-objective optimisation of wastewater treatment plant control to reduce greenhouse gas emissions. Water Res., 55, 52-62. DOI: 10.1016/j.watres.2014.02.018.

Tallec, G., Garnier, J., Billen, G., Gousailles, M., 2006. Nitrous oxide emissions from secondary activated sludge in nitrifying conditions of urban wastewater treatment plants: Effect of oxygenation level. Water Res. 40, 2972–2980. https://doi.org/10.1016/j.watres.2006.05.037

Tallec, G., Garnier, J., Billen, G., Gousailles, M., 2008. Nitrous oxide emissions from denitrifying activated sludge of urban wastewater treatment plants, under anoxia and low oxygenation. Bioresour. Technol., 99, 2200–2209; DOI: 10.1016/j.biortech.2007.05.025.

Wang, Y., Lin, X., Zhou, D., Ye, L., Han, H., Song, C., 2016. Nitric oxide and nitrous oxide emissions from a full-scale activated sludge anaerobic/anoxic/oxic process. Chemical Engineering Journal 289, 330–340. http://dx.doi.org/10.1016/j.cej.2015.12.074

Wisniewski, K., Kowalski, M., Makinia, J., 2018. Modeling nitrous oxide production by a denitrifying-enhanced biologically phosphorus removing (EBPR) activated sludge in the presence of different carbon sources and electron acceptors. Water Res., 142, 55-64; DOI: 10.1016/j.watres.2018.05.041.

Wunderlin, P., Mohn, J., Joss, A., Emmenegger, L., Siegrist, H., 2012. Mechanisms of N2O production in biological wastewater treatment under nitrifying and denitrifying conditions. Water Res. 46, 1027–1037. https://doi.org/10.1016/j.watres.2011.11.080

Yan, X., Han, Y., Li, Q., Sun, J., Su, X., 2016. Impact of internal recycle ratio on nitrous oxide generation from anaerobic/anoxic/oxic biological nitrogen removal process. Biochem. Eng. J. 106, 11–18; DOI: 10.1016/j.bej.2015.11.005.

Zaborowska, E., Czerwionka, K., Makinia, J., 2017. Strategies for achieving energy neutrality in biological nutrient removal systems – a case study of the Slupsk WWTP (northern Poland). Water Sci. Technol., 75, 727–740; DOI: 10.2166/wst.2016.564.